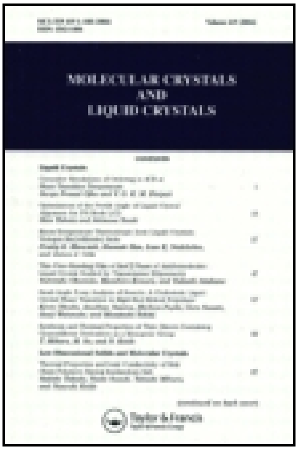

Molecular Crystals and Liquid Crystals

Intermolecular Embraces and Intermolecular Energies

Ian Dance [a]

[a] School of Chemical Sciences, University of New South Wales, Sydney, NSW, Australia

To cite this article: Ian Dance (2005): Intermolecular Embraces and Intermolecular Energies, Molecular Crystals and Liquid Crystals, 440:1, 265-293

To link to this article: http://dx.doi.org/10.1080/15421400590958593

Mol. Cryst. Liq. Cryst., Vol. 440, pp. 265–293, 2005
Copyright © Taylor & Francis Inc.
ISSN: 1542-1406 print/1563-5287 online
DOI: 10.1080/15421400590958593

Intermolecular Embraces and Intermolecular Energies

Ian Dance
School of Chemical Sciences, University of New South Wales,
Sydney, NSW, Australia

Control of the assembly of molecules in the crystalline state requires management of all possible intermolecular interactions, and their energies. Any one molecule is surrounded by and interacts with parts of the surface of several others, and it is the balance of all the intermolecular interaction energies that determines the lattice enthalpy, and therefore the product structure. In this context of competition between different intermolecular contacts, simplification occurs when intermolecular motifs operate in concert, as in multiple aryl embraces. Structural hierarchies of extended embrace motifs occur in crystals, analogous to the secondary ⇒ tertiary ⇒ quaternary construction of biological macromolecules. Some principles for the analysis and interpretation of intermolecular space in crystals are discussed.

Richly abundant data on the packing of molecules in crystals provides the basis for the description of intermolecular motifs, but this data is only geometrical. A different property, intermolecular energy, is determinative in the assembly of molecules. In strong contrast to the abundance of geometrical data, there is a serious scarcity of experimental thermodynamic data about many types of intermolecular motifs, including embraces. However, intermolecular potentials for chemically diverse systems can be calculated efficiently by appropriate density functional methods. Key concepts relating intermolecular potentials, the van der Waals distance criterion, and distributions of intermolecular distances, are reiterated. Charged polyatomic molecules, prevalent in coordination chemistry, raise significant questions about the relative magnitudes and influences of the additional electrostatic components of intermolecular energy. Some of the issues and uncertainties in this, for instance in the multiple phenyl embraces that occur between homocharged molecules, are discussed.

Keywords: aryl embrace motif; coordination complex; coulombic energy; crystal packing; intermolecular potential; polyatomic ion; van der Walls

This research is supported by the Australian Research Council, the University of New South Wales, and Australian Partnership for Advanced Computing. I thank my coworkers, Dr. Marcia Scudder and the students named in the references.

Address correspondence to Ian Dance, School of Chemical Sciences, University of New South Wales, Sydney, NSW 2052, Australia. E-mail: I.dance@unsw.edu.au

INTRODUCTION AND THEMES

This article is about the analysis and interpretation of the packing of molecules in crystals to gain understanding that can then be used in the design and, eventually, confident engineering of molecular crystals. I will include chemical systems that are more diverse than the normal gamut of the organic solid state [1,2]. In this research, the concepts and principles that are adopted influence the questions that are asked and investigated, and the progress made is determined by the incisiveness of the questions asked. Therefore, my goal in this article is to focus on some themes and issues which I believe to be broadly significant in the analysis, interpretation, and control of crystal packing.

An important underlying concept is that the formation of a molecular crystal from solution occurs with the testing of numerous possibilities for molecular aggregation, and therefore the resulting crystal structure is very likely to reveal a favourable arrangement, which is worth analysing to understand the principles involved. In this it is important to consider the complete structure of a molecular crystal, and all of intermolecular space, not just a preconceived intermolecular interaction or motif. It is also important to remember that a molecular crystal normally grows according to the sum of all energies involved (including desolvation energies which can influence growth morphology) [3].

This introduces at the outset the theme of intermolecular energy. Energy is a key property of molecular aggregation and the formation of molecular crystals. These energies are sometimes neglected, because information about them are less available, less precise, and less accurate than geometrical information available about crystal structure and intermolecular conformation. But neglect of energy is perilous if the goal is crystal engineering. Attempts to design and fabricate solid state materials using only an understanding of size and shape, without good knowledge of the energies involved, would be completely unacceptable in other fields of design and engineering.

This theme leads to a corollary theme, polymorphism. It is known for many molecular systems that more than one periodic arrangement can occur, and it is then usually presumed that these polymorphic crystals have similar lattice energies. This could be misconceived, because the polymorph formation may be kinetically controlled rather than thermodynamically controlled. At this point the repeatability of formation of a crystal structure is an important issue. On the basis of general experience many chemists (outside the pharmaceutical industry) have come to expect that their compound will crystallise the same way under different conditions, and to implicitly assume that the molecular packing observed in their crystal reflects the most favourable arrangement of intermolecular interactions. The literature is full of such single crystallisations, followed by diffraction measurements and subsequent serious interpretation of the crystal structure, without actually testing the repeatability. There is considerable reported experience that repeated crystallisations yield polymorphs, which are then much more informative than the original result. Given that repeated and alternative crystallisation procedures are often relatively straightforward experimentally (for the possessor of the compound), this testing is encouraged.

Two concepts developed in this article are structural hierarchies and energy hierarchies in crystal packing. In analysis of the geometrical relationships between molecules in a crystal, and in the design of molecular crystals, both of which necessarily aim for the complete crystal, the well-known hierarchy of secondary, tertiary and quaternary structure for biological macromolecules is a useful conceptual analogy. This thinking encompasses ideas about the repetition of favourable motifs, and the buildup from small to large units, to the complete entity. Examples of this approach for aryl embrace motifs are described below. Similarly, it is essential to appreciate the ranking of relative energies of intermolecular motifs as they contribute to the total lattice energy of a molecular crystal, and to recognise dominant energies. This is discussed later.

MULTI-COMPONENT CRYSTALS

The molecular biology analogy expands my thinking. Beyond the complete structure of a protein, enzyme, or nucleic acid, is the organelle, the operational unit. At this level many chemically different components are present, with defined roles. Molecular biology involves organised multi-component hetero-chemical matter. I ask, what would be the molecular crystal analog of the biological organelle? It would be a multi-component crystal, that is, a crystal that contains a substantial number of different molecules. But this is the antithesis of chemical crystallisation, where the objective is usually purification, the generation of a homo-chemical material from a hetero-chemical solution. Amongst the hundreds of thousands of molecular crystals in the Cambridge Structural Database (CSD) such multi-component crystals are very few, for the obvious reason that the solutions generating the crystals in the CSD generally contained few components. Nevertheless, it is challenging to think how crystals that contain, say, five or more large molecules could be generated. One reason for doing this would be to expand our appreciation of intermolecular interactions, which is restricted when dealing with the traditional molecular crystal.

One good example [4] of a crystal with four different and relatively large molecules is shown in Figure 1. Note that thinking about this

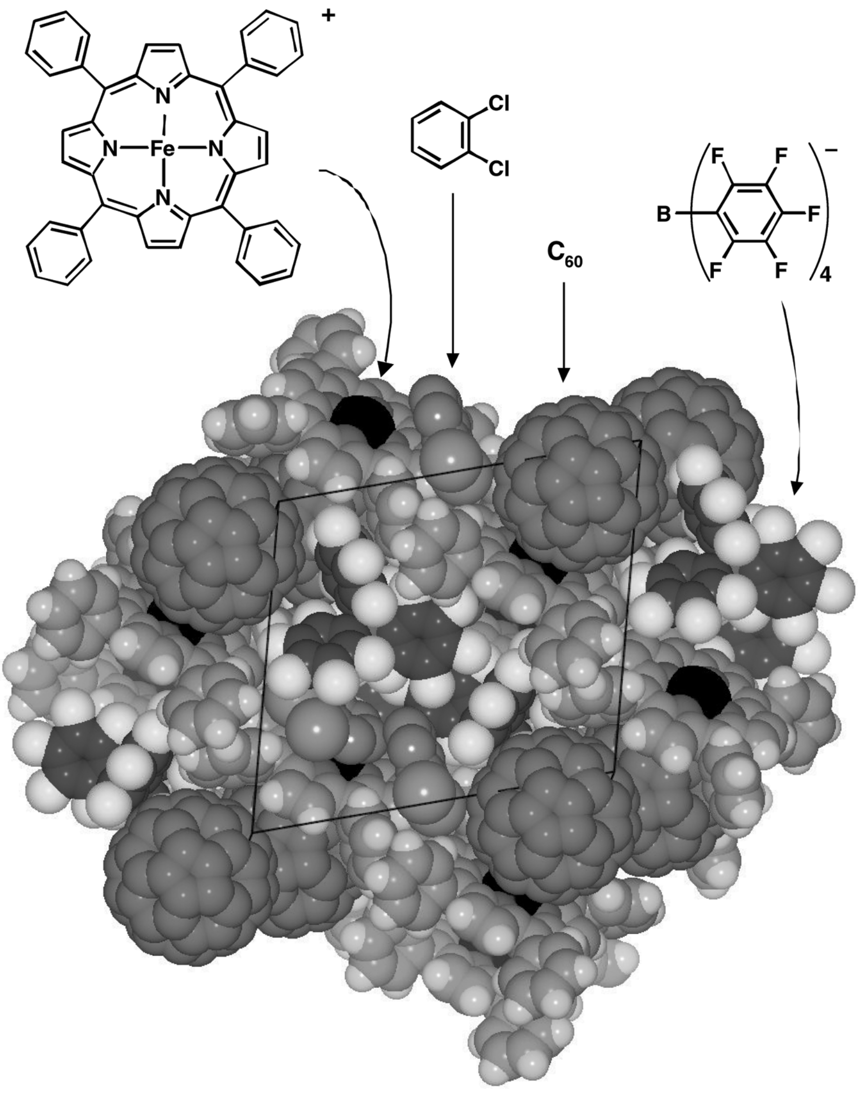

FIGURE 1 One of a few good instances of a multi-component molecular crystal [4].

multi-component crystalline molecular aggregate immediately focuses attention on the competitions and hierarchies of geometry and energy, which are the themes of this article.

In the CSD there are many crystals that contain a number of different solvent molecules. Solvent molecules are usually small: the question about solvent inclusion is often (a) whether it is a remnant manifestation of the solvation in the solution that yielded the crystal, or (b) whether the solvent molecule is filling a void caused by the arrangements of geometrically awkward molecules, or (c) whether the solvent contributes strong intermolecular energies, such as strong hydrogen bonding. One way to ensure at least a two-component crystal is to use charged molecules, i.e., large polyatomic ions. This necessarily raises the question of the relative magnitude of the electrostatic energies between polyatomic ions, a key question that is also discussed below.

EMBRACE INTERMOLECULAR MOTIFS

Embrace motifs have been developed principally for molecules that contain phenyl, aryl, or heteroaryl appendages. Isolated aromatic molecules engage in the well-known offset-face-to-face (OFF) and edge-to-face (EF) primary motifs [5], illustrated in Figure 2(a) for a pair of benzene molecules. When part of a larger molecule these aryl components have some conformational restrictions, and where there are multiple aryl substituents there is the possibility of concerted formation of intermolecular OFF and/or EF primary motifs, generating a secondary embrace motif. Figure 2(b) shows the (OFF)(EF)$_2$ embrace occurring between a pair of Ph_4P^+ ions, and Figure 2(c) shows the analogous embrace between a pair of $[M(phen)_3]^z$ metal complexes (phen = 1,10-phenanthroline).

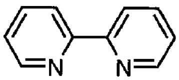

bipy

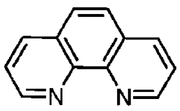

phen

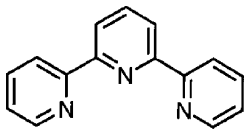

terpy

The essential character of embraces is concerted operation of primary motifs to generate a secondary, larger intermolecular motif. These are named embraces because they are multi-armed, mutual, and attractive (at least for the van der Waals component of intermolecular energy).

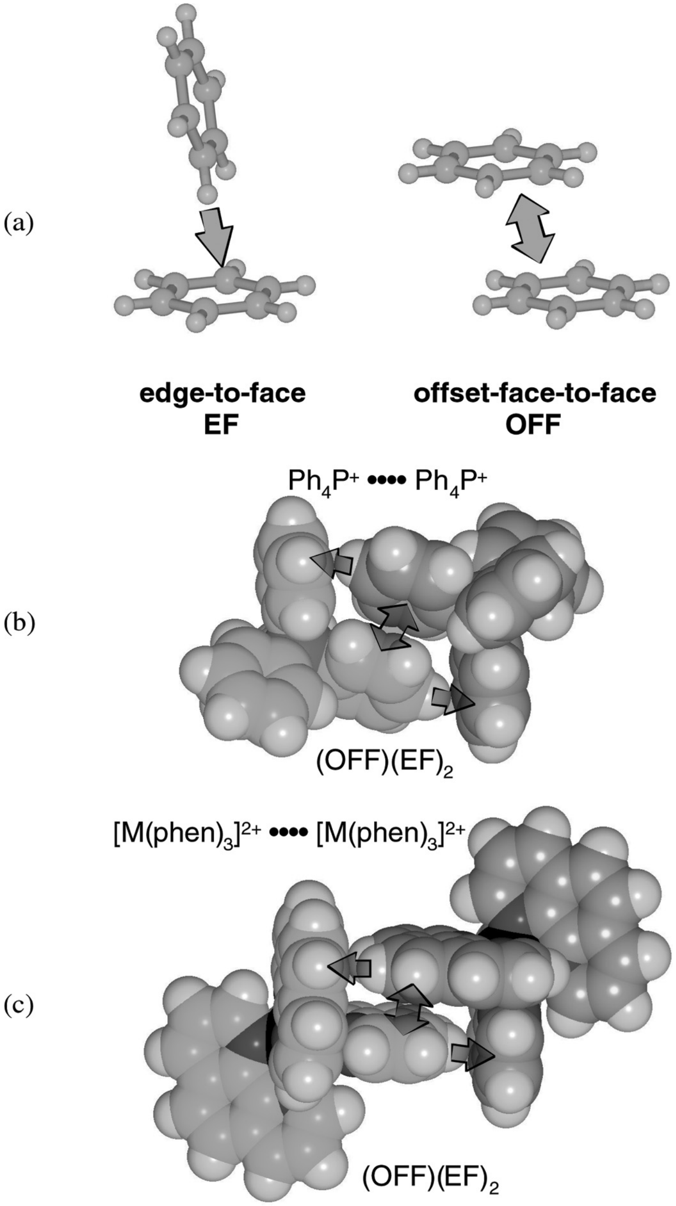

FIGURE 2 (a) The primary edge-to-face and offset-face-to-face interactions of aromatic molecules and substituents. (b) The centrosymmetric (OFF)(EF)$_2$ embrace between a pair of Ph_4P^+ ions. (c) The centrosymmetric (OFF)(EF)$_2$ embrace between a pair of $[M(phen)_3]^z$ metal complexes. The single arrow (EF) and double arrow (OFF) symbols are used in subsequent figures.

The sixfold aryl embrace is six aromatic entities engaged in a concerted cycle of six EF primary motifs. Figure 3(a) shows a pair of $Ph_3POGaCl_3$ molecules, of opposite chirality, facing each other across a centre of inversion such that there is a cycle of six EF primary motifs (marked with arrows) directed back and forth between the Ph_3P faces of the molecules (which are distinguished by colour of the C atoms). The Ph_3E moiety (E = group 14,15 elements) needs threefold rotor conformation to form this sixfold phenyl embrace $(EF)_6$ embrace. Octahedral metal complexes with three bidentate heteroaromatic ligands, such as $[M(bipy)_3]^z$ (bipy = 2,2′-bipyridine) present a threefold rotor array of pyridyl groups, and so can form the same $(EF)_6$ embrace, which is shown in Figure 3(b).

Embracing molecules can associate further, in additional embraces, and thereby progress up the structural hierarchy. Figure 4(a) shows part of an infinite chain of $[M(bipy)_3]^z$ complexes, all linked by $(EF)_6$ embraces. This is possible because $[M(bipy)_3]^z$ complexes present the threefold rotor conformation of pyridyl groups at both ends [6]. These chains, which now represent a tertiary level of structure for molecular association, occur in a number of crystals, and notably in the crystal structures of $[Ru(bipy)_3]^0$, $[Ru(bipy)_3]^{2+}(PF_6^-)_2$, and $[Ru(bipy)_3]^{3+}(PF_6^-)_3$ where the crystals are comprised of parallel chains. Figure 4(b) shows projections along the infinite chains of sixfold aryl embracing cations in $[Ru(bipy)_3]^{2+}(PF_6^-)_2$ [6], and $[Fe(phen)_3]^{2+}$ I_6^{2-} [7].

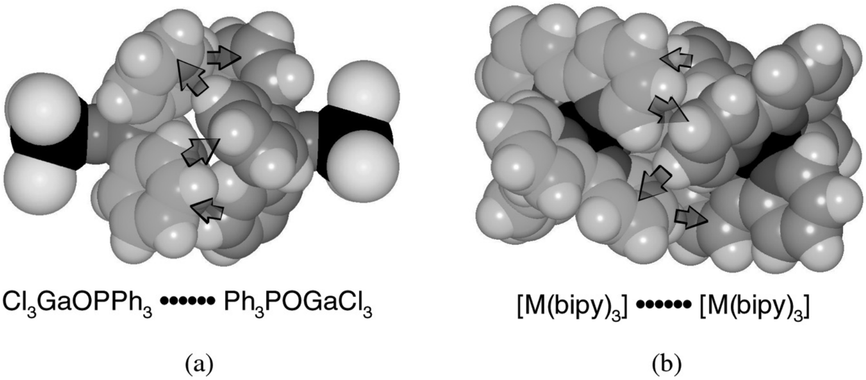

FIGURE 3 (a) The sixfold phenyl embrace between a pair of enantiomeric $Ph_3POGaCl_3$ molecules. (b) The sixfold aryl embrace between a pair of $M(bipy)_3]$ complexes. In both figures two of the arrows indicating the cyclic set of $(EF)_6$ interactions are obscured behind.

Molecules Ph_4E, including the common cation Ph_4P^+, use three of the four phenyl groups to form the sixfold phenyl $(EF)_6$ embrace (Fig. 3(a)), but there are three other Ph_3E set in the molecule. By use of more than one set of three Ph groups, these molecules can form more than one $(EF)_6$ embrace, as illustrated in Figure 5(a). The tetrahedral stereochemistry of Ph_4E requires that the chain is zig-zag, and this tertiary motif has been named the zig-zag sixfold phenyl embrace [8]. This motif occurs in a large number of crystals containing the Ph_4P^+ cation, and one example, $(Ph_4P^+)_2$ $[Mo_6O_{19}]^{2-}$ $(CH_3CN)_2$ [9], is shown in Figure 5(b).

Molecules Ph_4E can also form an $(EF)_4$ embrace, involving two phenyl rings from each molecule (see Fig. 6(a)). The relationship between the two molecules is simply translation, and so this embrace can be repeated by translation (progression from secondary to tertiary structure), and linear chains of Ph_4P^+ cations occur in many crystals: one example is shown in Figure 6(b).

In the structural hierarchy of intermolecular motifs, the crystal structures shown in Figures 4(b), 5(b) and 6(b) are examples of the tertiary level. Another variant of tertiary association occurs for octahedral metal complexes $[M(terpy)_2]^z$, which form pairwise secondary embrace motifs $(OFF)(EF)_2$ like that of Figure 2(b), which then repeat in two-dimensions to generate tertiary "terpy embrace" layers [2,10].

These patterns of multiple aryl embraces are established because the molecules involved, such as Ph_4P^+, and metal complexes with bipy,

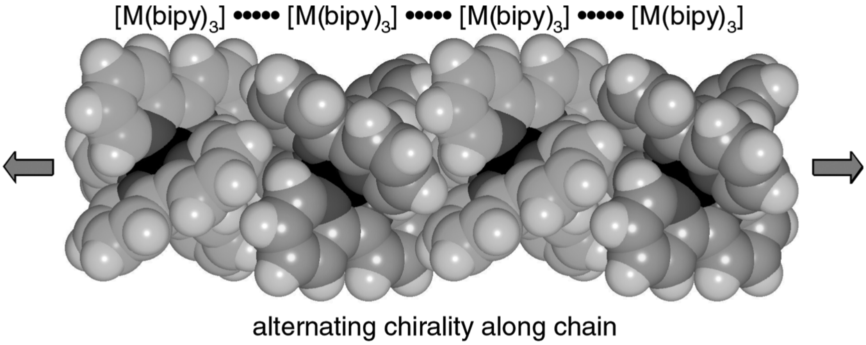

FIGURE 4 (a) The infinite chain of sixfold aryl embracing $[M(bipy)_3]$ complexes, with alternating chirality along the chain. (b) Projections along these chains as they occur in $[Ru(bipy)_3]^{2+}(PF_6^-)_2$ (upper) and $[Fe(phen)_3]^{2+}I_6^{2-}$ (lower).

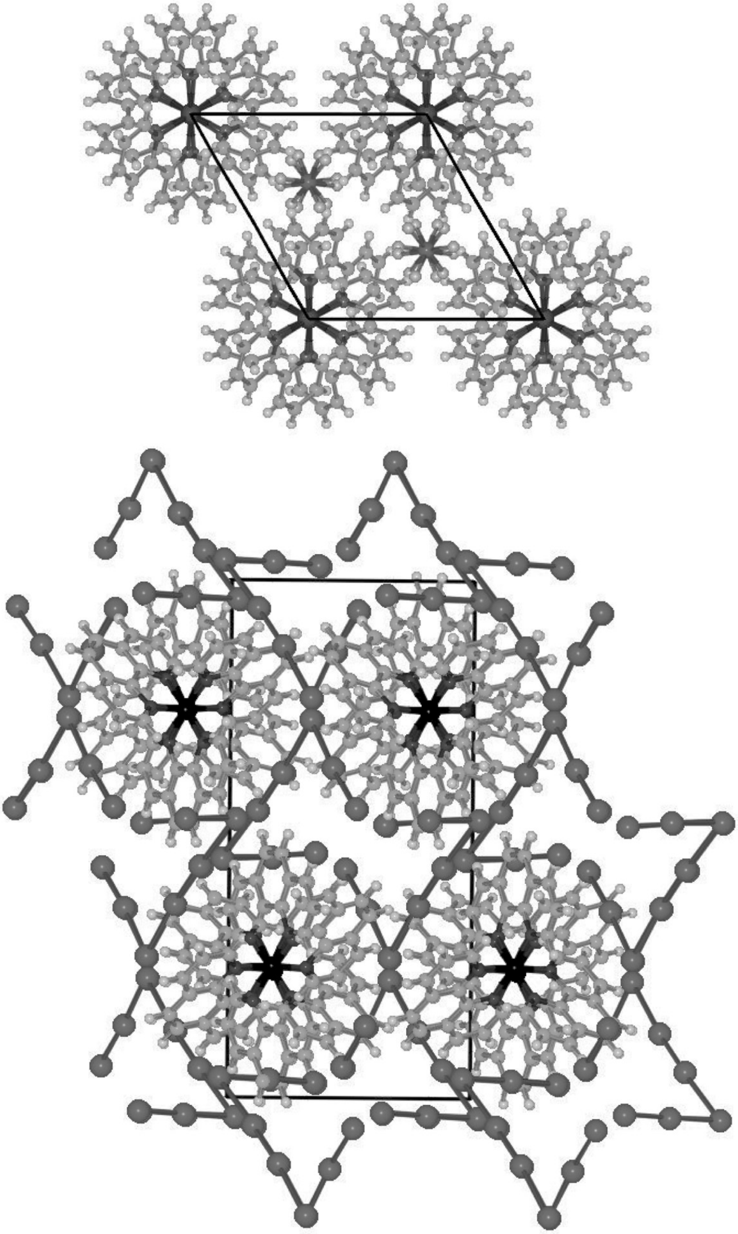

(b)

FIGURE 4 Continued.

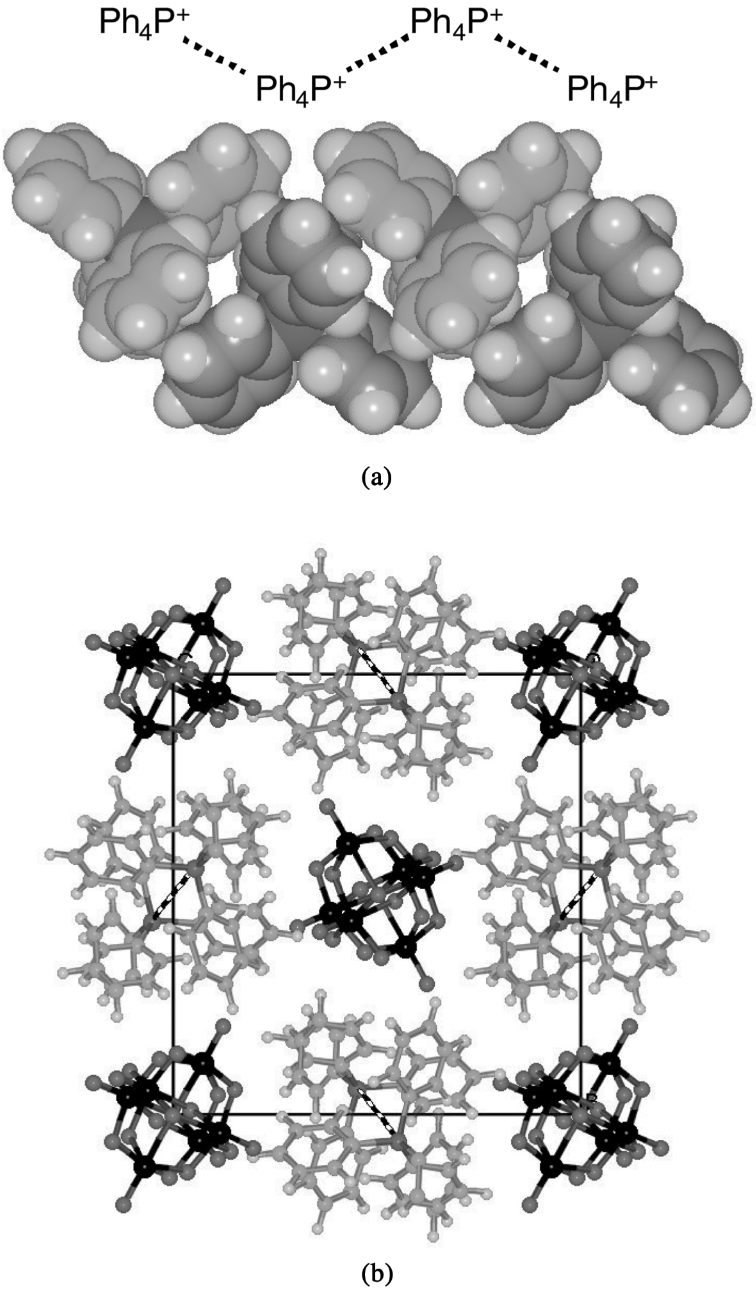

FIGURE 5 (a) A zig-zag chain of Ph_4P^+ ions, each engaged in two sixfold phenyl embraces with neighbours. All P atoms occur in the same plane, and therefore the end-view of the chain appears as in (b) where the dotted line is the projection of the P**...**P embrace vectors. (b) is a projection of the crystal structure of $(Ph_4P^+)_2\ [Mo_6O_{19}]^{2-}\ (CH_3CN)_2$.

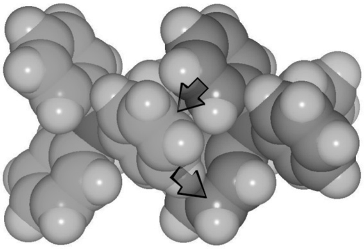

(a)

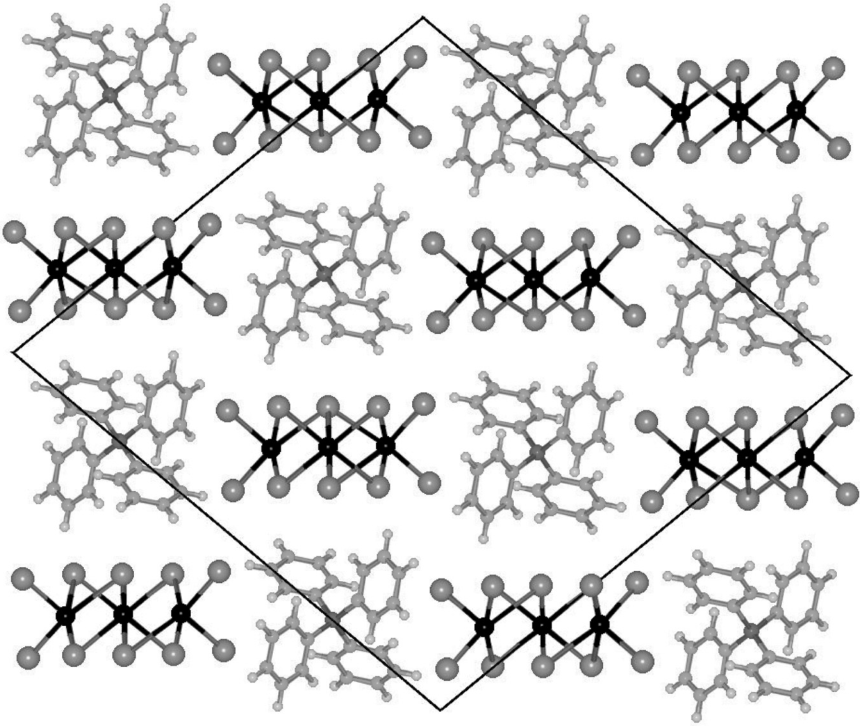

(b)

FIGURE 6 (a) The fourfold $(EF)_4$ embrace between a pair of Ph_4E molecules: two of the arrowed EF interactions are obscured behind. (b) A projection of the crystal structure of Ph_4P^+ $[Sb_3I_{10}]^-$ (Sb black, I orange): the apparently single cations are in fact chains linked by $(EF)_4$ embraces and related by crystallographic translation along the projection direction.

phen and terpy ligands, are common and have been used in synthesis and crystallisation by many researchers.

The next level in the structural hierarchy of embrace motifs is quaternary. It occurs when the tertiary chains and layers are linked further by embraces. A number of these structures have been recognised and described [11,12]. One of them is elaborated in the next section.

HIGH-SYMMETRY CRYSTALS CONTAINING EMBRACES

The $(EF)_6$ embrace already described can have $\bar{3}$ symmetry. When threefold symmetry occurs in the complete molecule that is engaged in this threefold embrace there is the possibility of building high symmetry crystal lattices, a possibility that is realised in a number of intriguing crystal structures. A commonly occurring hexagonal lattice type is illustrated in Figure 7 with the Ph_3PMe^+ cation. A variety of molecules form this three-dimensional array of $(EF)_6$ embraces [11]: some examples are listed in Table 1.

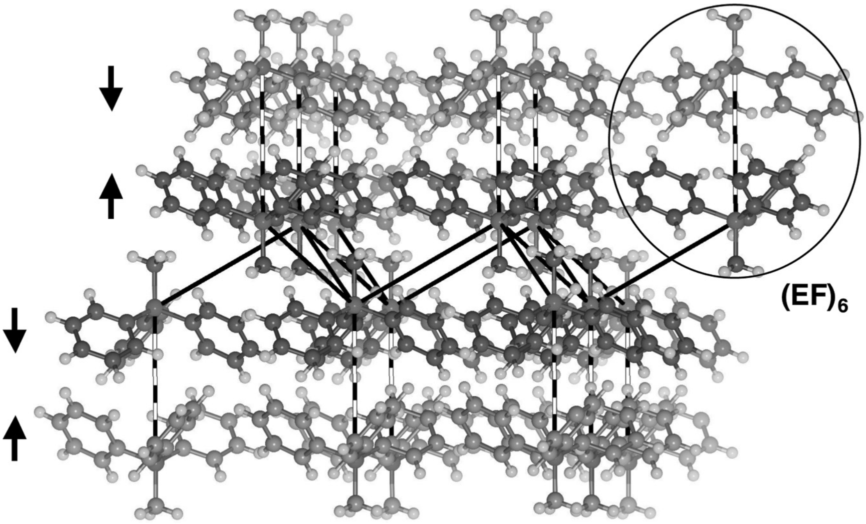

FIGURE 7 Part of the hexagonal lattice of $(EF)_6$ embraces between Ph_3PMe^+ cation: P, magenta; C, green/brown; H, cyan. Each embrace (with $\bar{3}$ symmetry) involves green and brown cations, and is marked with black and white striped rods. Cations are arranged in puckered hexagonal nets, one of which is outlined with black rods. This example is from the crystal structure of $(MePh_3P^+)_2\,[Cu_2Br_5]^{2-}$ [13], in space group $R\bar{3}c$: the $[Cu_2Br_5]^{2-}$ anions, not shown, are located at the centres of a puckered hexagons of cations involved.

TABLE 1. Molecules that Crystallise with the Hexagonal Array of $(EF)_6$ Embraces

$(MeOC_6H_4)_3As$
$(C_6F_5)_3B{-}PH_3$
$Ph_3C{-}COOH$
$(C_6F_5)_3Ge{-}GeEt_3$
$Ph_3PO{-}AlMe_3$
$(Ph_3PH^+)_2\ [Ga_2Cl_6]^{2-}$
$(Ph_3PCl^+)_2\ [MoCl_6]^{2-}$
$(Ph_3PMe^+)_2\ [Cu_2Br_5]^{2-}$
$Ph_3P{-}Au{-}V(CO)_6$
$Ph_3Si{-}O{-}TiN(CH_2CH_2O)_3$
$Ph_3P{-}Cu{-}(\mu{-}SPh)_3{-}U{-}(\mu\text{-}SPh)_3{-}Cu{-}PPh_3$
$Ph_3Si{-}N{=}C{=}N{-}SiPh_3$
$(MeC_6H_4)_3Pb{-}Sn(C_6H_4Me)_3$

This lattice type demonstrates the principle of frequent repetition of a favourable motif, to build up the complete crystal lattice. This principle is manifest in some other high symmetry lattices [14], three of which are illustrated in Figure 8. In $Ph_3P{=}N{=}PPh_3^+$ $[Nb(CO)_6]^-$, in the rhombohedral space group $R\bar{3}$, bimolecular $(EF)_6$ embraces like those just described do not occur, but instead a larger concert of primary motifs, hexamolecular $(EF)_6(OFF)_6(EF)_6$ (Fig. 8(a)). The molecule Ph_3AsI_2 crystallises in a cubic space group, $Pa\bar{3}$, using the conventional bimolecular $(EF)_6$ six-fold phenyl embrace. Molecules form chains$\cdot I{-}I{-}AsPh_3\cdot\cdot Ph_3As{-}I{-}I\cdot\cdot\cdot I{-}I{-}AsPh_3\cdot\cdot Ph_3As{-}I{-}I\cdot\cdot$ along all threefold axes of the cubic cell, as illustrated in Figure 8(b). Crystalline $Ph_3P{-}Au{-}CC{-}Au{-}PPh_3\ (C_6H_6)_2$ also crystallises in space group $Pa\bar{3}$, but without the bimolecular $(EF)_6$ embrace, because the chains of molecules along all threefold axes of the cell are interrupted by benzene molecules: $\cdot Ph_3P{-}Au{-}CC{-}Au{-}PPh_3\cdot\cdot C_6H_6\cdot\cdot Ph_3P{-}Au{-}CC{-}Au{-}PPh_3\cdot$. Instead there are hexamolecular $(EF)_6$ embraces, surrounding all threefold axes of the cube (Fig. 8(c)).

These high symmetry crystals are formed by molecular compounds, and are unlike the majority of high symmetry crystal lattices which are comprised of monatomic or small inorganic ions, in *non*-molecular solids. In order to achieve high symmetry crystallisation of polyatomic ions, one of the requirements is a favourable symmetric intermolecular motif, which is repeated because it is energetically favourable.

Note that when we consider the complete set of intermolecular interactions for these molecules, we determine and then examine the asymmetric unit of intermolecular space as well as the asymmetric section of the molecule.

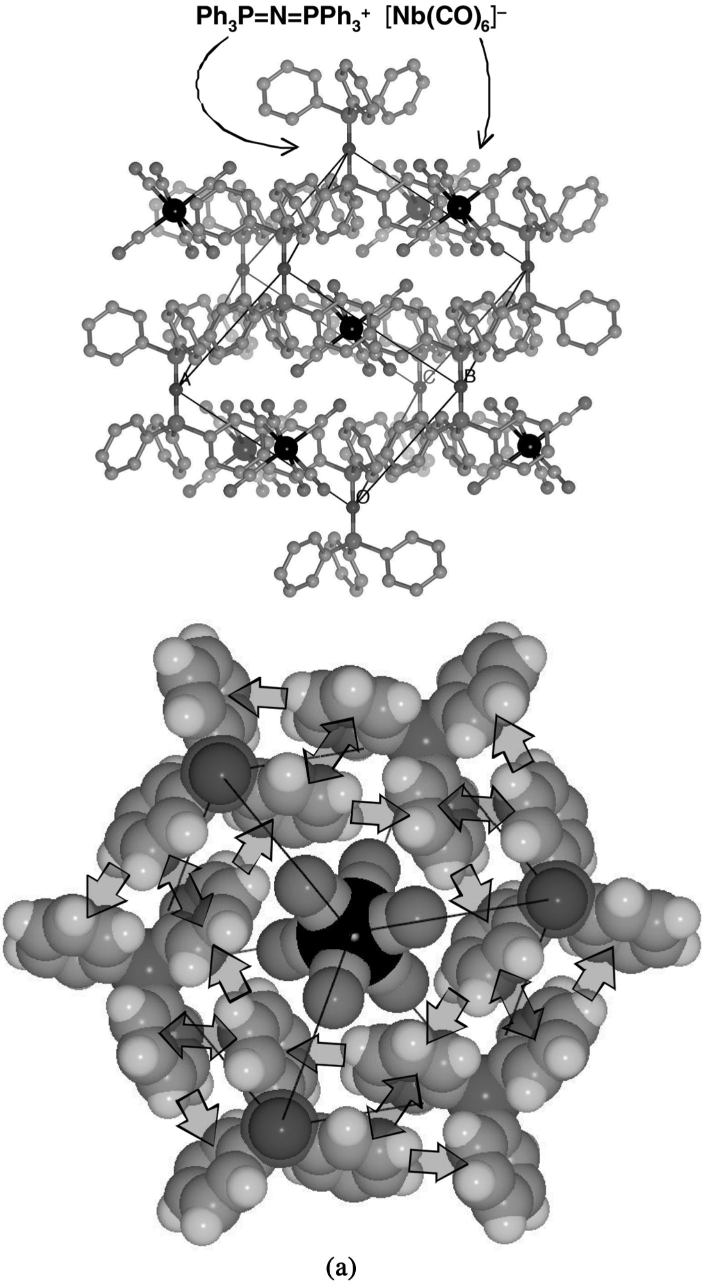

FIGURE 8 Continued.

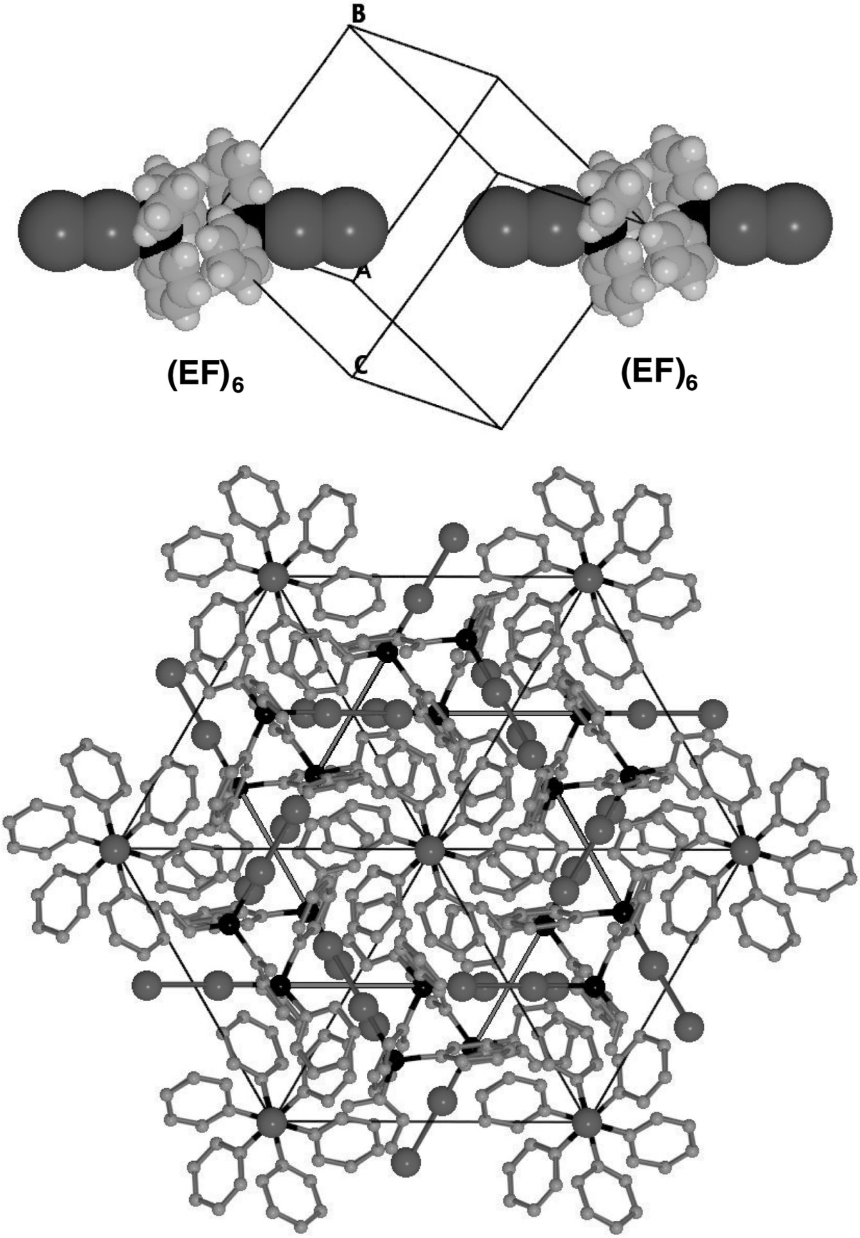

(b)

FIGURE 8 Continued.

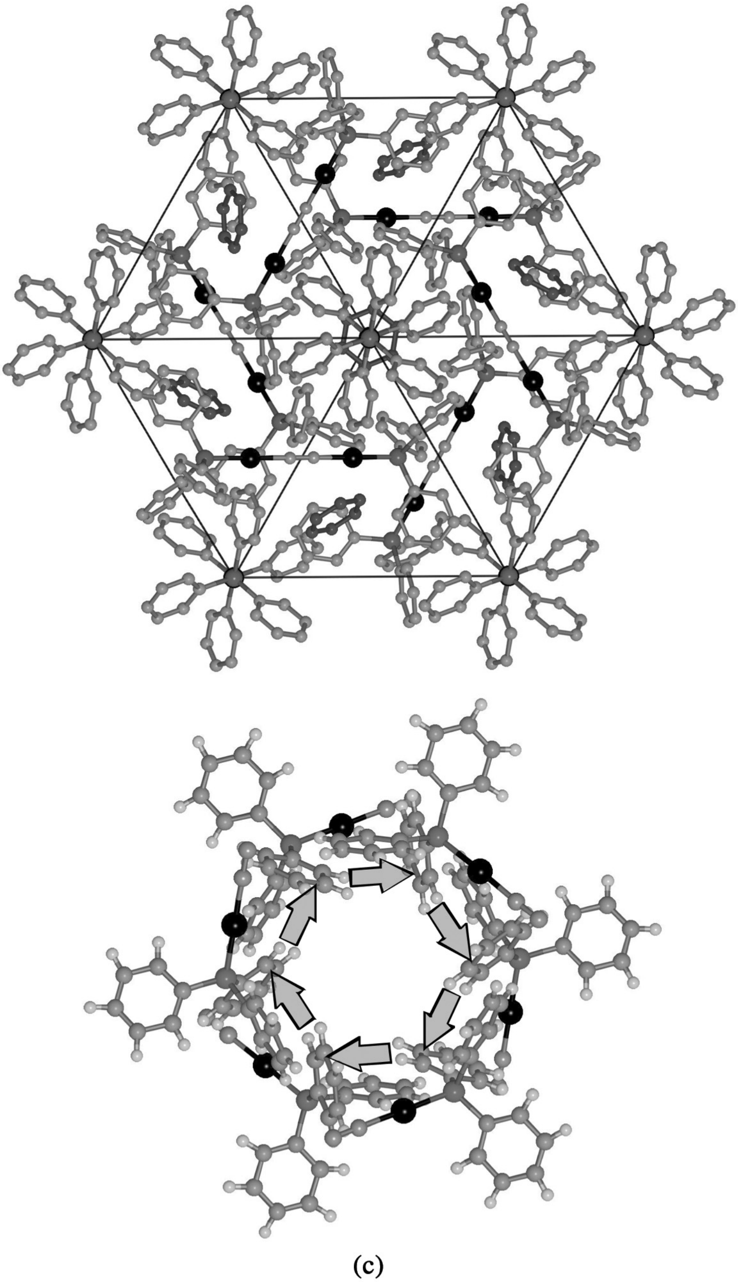

FIGURE 8 Continued.

SYMMETRY AND CRYSTAL PACKING ANALYSIS

This adherence to the principle of assessing all intermolecular space becomes relatively simple in these high symmetry examples. It does however draw attention again to the conceptual basis for crystal packing analysis, illustrated in Figure 9. There is the molecule and its (point group) symmetry, which can introduce the concept of an asymmetric segment of a symmetrical molecule. Then there is the intermolecular space around the molecule, and the asymmetric unit of that space. If there is a cavity that may or may not contain other species (as in Fig. 7, Fig. 8(a), (c)), the symmetry and asymmetric sector of the cavity need to be considered. These combine in the crystal symmetry (space group) and its familiar asymmetric unit. The analysis of crystal packing, particularly when the goal is interpretation of intermolecular interactions, requires identification of both the molecule(s) and the intermolecular space that is propagated by the space group symmetry.

These principles apply similarly to low symmetry crystals, and to crystals where the absence of symmetry in intermolecular space leads to more than one molecule in the asymmetric unit, molecules where $Z' > 1$. This has been discussed recently by Steed [15]. An extreme example is crystalline $ReCl_2(PMe_3)_2(NO)(NCMe)$, which contains 11 of these relatively small molecules in the crystallographic asymmetric unit [16]. My interpretation here is that there is such variety of (equienergetic) intermolecular interactions at the diverse surface domains of this molecule that the aggregate of unique intermolecular space is

◀

FIGURE 8 Three high symmetry crystal structures that are constructed by multiple repetition of favourable embrace motifs. (a) $Ph_3P{=}N{=}PPh_3^+$ $[Nb(CO)_6]^-$, in the rhombohedral space group $R\bar{3}$, has cations and anion alternating along the trigonal axis and no bimolecular $(EF)_6$ secondary motifs: Nb, black; CO, orange-red; P, magenta; N, blue. The lower figure shows the hexamolecular concert, $(EF)_6(OFF)_6(EF)_6$, of six $Ph_3P{=}N{=}PPh_3^+$ ions surrounding a $[Nb(CO)_6]^-$ ion: EF, red arrows; OFF, blue arrows. Three of the $Ph_3P{=}N{=}PPh_3^+$ ions, pointing upwards, have been truncated at N to clarify the picture. (b) The cubic crystal structure of Ph_3AsI_2 (space group $Pa\bar{3}$). The chains of molecules connected by bimolecular $(EF)_6$ embraces shown in the upper section are repeated along all of the threefold axes of the cell, as shown in the lower picture. (c) The cubic crystal structure of $Ph_3P{-}Au{-}CC{-}Au{-}PPh_3\ (C_6H_6)_2$ (space group $Pa\bar{3}$: central −CC −coloured orange, benzene molecules blue) contains hexamolecular $(EF)_6$ embraces (red arrows). Benzene molecules encircle the threefold axes and interrupt bimolecular $(EF)_6$ embraces. In the lower section one $AuPPh_3$ part of each of the six molecules is not shown.

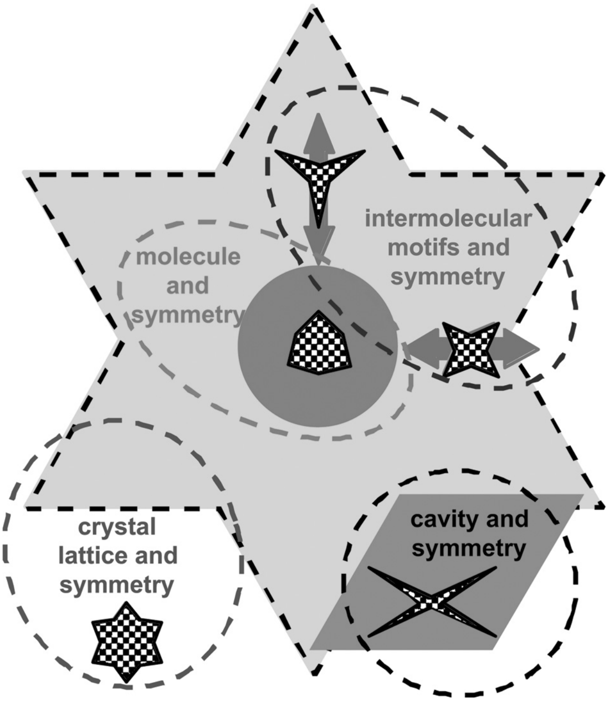

FIGURE 9 Diagrammatic representation of the concepts of entities and symmetries for molecular crystals. The checkered images are icons for different aspects of the symmetry. The familiar crystal symmetry (space group) (blue) is comprised of the molecule and its (possible) asymmetric segment (red), the intermolecular space (green) possibly containing symmetry elements and having an asymmetric unit, and the symmetry and asymmetric sector of any cavities and their contents (black).

large enough to envelope 11 molecules. Put differently, it takes 11 molecules and many different intermolecular domains to manifest all of the approximately equi-energetic intermolecular motifs.

→

FIGURE 10 Key relationships between intermolecular energy (black curves), distributions of interatomic distance across the immediate intermolecular space (blue curves), and the van der Waals distance. (a) is the standard van der Waals potential: the van der Waals distance is *ca.* 0.4 Å shorter than the distance for maximum intermolecular stabilisation and the peak in the distribution of intermolecular distances; stabilising interactions in the green range outweigh the fewer destabilising interactions in the red range. (b) represents the closer potential when there are Lewis acid–base functions, or strong hydrogen bonding, and/or charge assistance from oppositely charged ions.

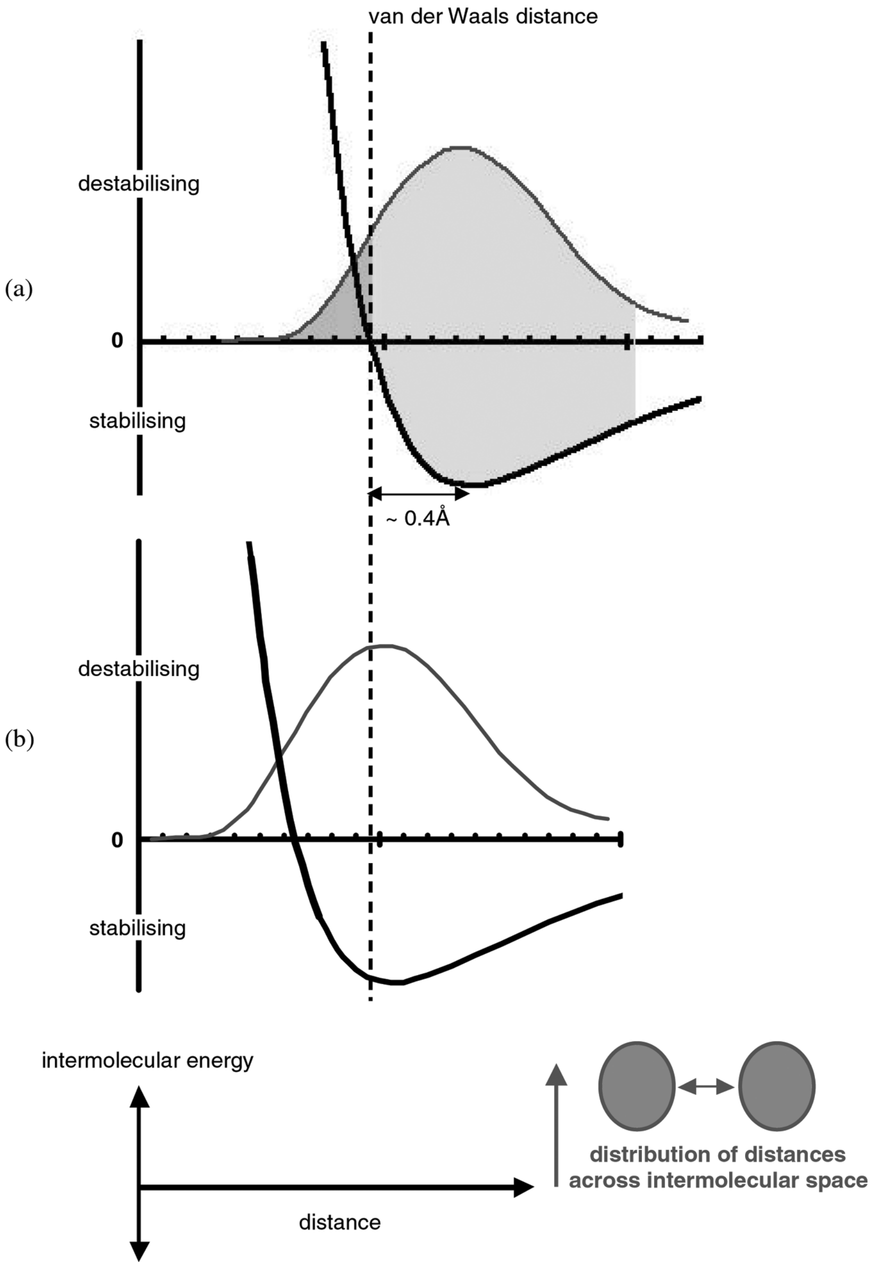
van der Waals distance
destabilising
(a)
0
stabilising
~ 0.4Å
destabilising
(b)
0
stabilising
intermolecular energy
distance
distribution of distances
across intermolecular space

Crystal polymorphs are crystal packing isomers. In this sense, crystals with large Z′, such as that just mentioned, could be regarded as having a number of polymorphs in the one crystal!

INTERMOLECULAR ENERGIES

Conceptual Bases: Intermolecular Potentials and Distances

Energies, not geometries, are determinative in the packing of molecular crystals. It is ironic that while there is available an impressive abundance of geometrical data about intermolecular phenomena, there is a serious general scarcity of experimental energy data. Some motifs, like hydrogen bonds, have been measured and energy data are available [17], but for most interactions there is not much relevant energy data. The molecule $ReCl_2(PMe_3)_2(NO)(NCMe)$, just mentioned as probably engaging in a number of equi-energetic intermolecular motifs, highlights the uncertainty about what those energies may be, due to lack of experimental data.

We can tackle this deficiency in two ways. One is to use theoretical calculations of intermolecular energies, and the other is to develop the relationships between geometry and energy—intermolecular potentials—so that the abundant geometrical data can be better translated into energy information. I will discuss both of these approaches, firstly reviewing the key principles for intermolecular potentials [2], and the commonly used van der Waals criterion [18].

Figure 10(a) shows a representative atom–atom potential (energy vs. distance) for a van der Waals intermolecular interaction. Negative energies are stabilising: positive energies at short distance are destabilising: note that the adjectives "attractive" and "repulsive", which describe force and refer to the slope of the potential, are less relevant. The potential has a broad stabilising region (shaded green in Fig. 10 (a)) extending over *ca.* 1 Å, but then rises more sharply (depending on the polarisability of the atoms involved) to strong destabilisation at shorter distances. In general the distance domain of the stabilising region of the intermolecular potential is approximately double the bond distance between the same atom types. Figure 10(a) also shows the generalised distribution of interatomic distances across the immediate intermolecular space (obtained from the distribution of all intermolecular interatomic distances by subtraction of the general cubic increase of volume expansion) [18]. As expected, the distribution of distances reflects, approximately, the intermolecular potential. The majority of intermolecular distances occur where the stabilising energy is greatest. The bottom of the intermolecular potential is a significant distance criterion for the atom types involved.

Intermolecular distances are normally referenced to the van der Waals distance (sum of the van der Waals radii), and so it is important to know how this distance relates to the intermolecular potential. As marked on Figure 10(a), the van der Waals distance occurs where the intermolecular energy is close to zero, or slightly positive, which is also part way up the leading edge of the distribution of distances [18,19].

A number of key concepts are relevant here [18]. One is that the influential intermolecular distances, those that provide the cohesive energy, are appreciably longer than the van der Waals distance: I have estimated that, in general, the bottom of the potential well for van der Waals interactions occurs at a distance *ca*. 0.4 Å longer than the van der Waals distance. The important region responsible for the aggregation of molecules occurs over a broad range. The second key concept is definition of van der Waals contact, as the closest contact that does not cause destabilisation: the energy is close to zero at this van der Waals contact distance. Intermolecular distances less than the van der Waals distances are destabilising, and are a small minority in the distribution of distances. A third key general concept for crystal packing of molecules is that a larger proportion of more stabilising interactions, longer than the van der Waals distance (green in Fig. 10(a)), can impose a small proportion of destabilising interactions, less than the van der Waals distance (red in Fig. 10(a)). Fourthly, in the vicinity of the van der Waals distance, shorter is not stronger: longer is stronger (contrary to the normal concept for intramolecular bonding).

When the surfaces of molecules have chemical functionalities that can engage in specific intermolecular interactions, this picture can be modified. Lewis acid/Lewis base interactions and strong hydrogen bonds are the common instances of these additional interactions. Electrostatic interactions, for molecules with strong multipoles, or for charged molecules, also have enhanced intermolecular stabilisations: in the case of polyatomic ions these intermolecular energies are much larger, as described below. Charge transfer interactions are also stabilising. The general effect of these additional intermolecular stabilisations is a shift of the intermolecular potential and the associated distance distribution to shorter distances, as illustrated in Figure 10(b). Now the van der Waals distance is located within the stabilising well of the intermolecular potential, and nearer the top of the distance distribution, and distances less than the van der Waals distance may indicate stronger interactions.

The conceptual framework outlined above provides a general basis: the diversity of surfaces and shapes in molecules (particularly inorganic molecules) introduces many specific considerations.

Calculations of Intermolecular Potentials

Empirically parametrised analytical expressions are commonly used where molecules contain standard functionalities. Key issues for these methods are the validity of the atom type parameters used, and the treatment of electrostatic intermolecular interactions. Electrostatic intermolecular energies calculated in this way are strongly dependent of the assignment of atom partial charges, and the choice of permittivity for the intervening space.

Quantum methods do not have these uncertainties, and accommodate chemical diversity, but are quite severely restricted by the computational resources required. I use a density functional (DF) method, which has at least an order of magnitude advantage in computational speed over correlated Hartree-Fock methods. Further, I use numerical basis sets, calculated over a large grid, which avoid the issue of basis set superposition error associated with Gaussian basis sets [20]. This methodology is implemented in the program DMol of Bernard Delley [20,21]. Selection of functional is a vital aspect of DF calculations: the gradient corrected functionals that are suitable for calculation of intramolecular properties are demonstrably inadequate for weak intermolecular interactions [22]. The local density functionals are suitable, and the Perdew-Wang functional known as pwc [23] provides acceptable results. In calculations to validate these methods, against the experimental intermolecular potentials for Ar•••Ar and Xe•••Xe, and the intensely studied pair of benzene molecules, it was found that the pwc functional gives good account of the Xe•••Xe and benzene•••benzene potentials: there is a small overestimate of the intermolecular energy and small distance contraction of the potential well [2].

The advantage of the DMol methodology is computational efficiency, and so, with cognisance of the small overestimation by the pwc functional, it can be applied to secondary intermolecular motifs, and higher. Figure 11(a) shows the calculated (pwc) intermolecular potential for a pair of $[Ru(bipy)_3]^0$ complexes, engaged in the $(EF)_6$ embrace of Figure 3(b). The energy well occurs at Ru–Ru = 7.2 Å, while in crystalline $[Ru(bipy)_3]^0$ this distance is 7.7 Å. Part of this difference is caused by the calculation for just a pair of molecules, while the experimental distance is for the crystal phase where the intermolecular stabilisation energies are distributed isotropically and can be diminished relative to the anisotropic pair. The difference is also due in part to the over-estimation by pwc. The intermolecular energy of this embrace, *ca.* 15 kcal mol^{-1}, is consistent with the *ca.* 2 kcal mol^{-1} for a benzene pair: six pyridyl EF pairs are

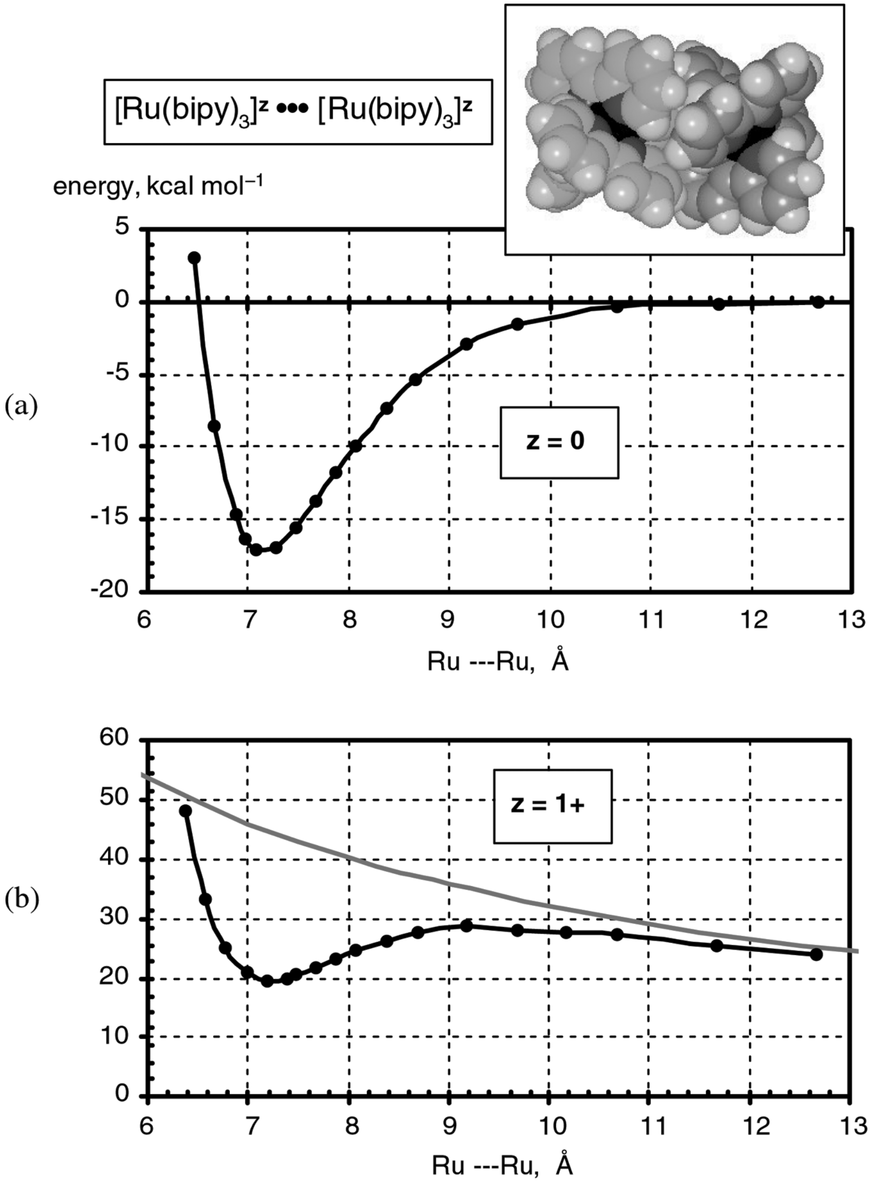

FIGURE 11 Intermolecular potentials for the sixfold $(EF)_6$ embrace between a pair of $[Ru(bipy)_3]^z$ complexes, for $z = 0$ and $z = 1+$, calculated by the density functional method with the pwc functional and numerical basis sets. The red curve is the coulombic energy for 1+ charges at the Ru centres, with permittivity $\varepsilon = 1$.

directly involved in the $[Ru(bipy)_3]^0 \cdots [Ru(bipy)_3]^0$ embrace. Note that the *intermolecular* potential for polyatomic molecules, Figure 11(a), has the same general shape as the *interatomic* potentials, and is relatively soft with a half-depth span of at least 1.5 Å.

Intermolecular Energies For Charged Polyatomic Molecules

At this point I consider the fact that a large number of the embracing molecules already described are polyatomic cations, between which electrostatic destabilisation would be expected. These homocharged molecules clearly associate in crystals. One issue is the extent to which the electrostatic destabilisation counteracts the underlying van der Waals stabilisation: what are the relative magnitudes of the energies (and distance dependences) of these two components of the interaction, for homo-charged and hetero-charged polyatomic ions?

Figure 11(b) shows the calculated potential for a pair of $[Ru(bipy)_3]^+$ complexes in the same $(EF)_6$ embrace. The energy is positive (destabilising) throughout the distance range, with a local minimum of $+20$ kcal mol^{-1} at Ru–Ru $= 7.3$ Å. Also marked on Figure 11(b) is the coulombic energy for a pair of positive charges at the Ru centres (with permittivity $\varepsilon = 1$), and the calculated potential approaches this asymptotically at long distance. The interpretation of the calculated potential as the combination of the electrostatic coulombic energy and the van der Waals stabilisation energy is evident in that the calculated total potential for $[Ru(bipy)_3]^+ \cdots [Ru(bipy)_3]^+$ is approximately the sum of the $+ \cdots +$ coulombic energy and the potential for $[Ru(bipy)_3]^0 \cdots [Ru(bipy)_3]^0$ in Figure 11(a). While this is a simplified interpretation, because the electrostatic energy for the pair of charged molecules will differ from the coulombic point charge energy at observed distances, it is useful. As illustration of this, the calculated potential for doubly charged complexes $[Ru(bipy)_3]^{2+} \cdots [Ru(bipy)_3]^{2+}$ (not shown) is again approximately the sum of the coulombic energy ($+170$ kcal mol^{-1} at 7.5 Å) and the van der Waals stabilisation. Further details and discussion will be published separately.

How can we reconcile the fact that innumerable crystals contain embracing polyatomic cations, and some crystal lattices are seemingly built from cations (for example Fig. 7), yet the intermolecular energies between these polyatomic cations are destabilising? The answer lies with the counter ions, which bring substantial electrostatic stabilisation to a crystal comprised of polyatomic ions. Figure 12 illustrates diagrammatically the potentials and the relative magnitudes of energy contributions for a polyatomic monocation and monoanion. While the coulombic components are equal and opposite for homo- and

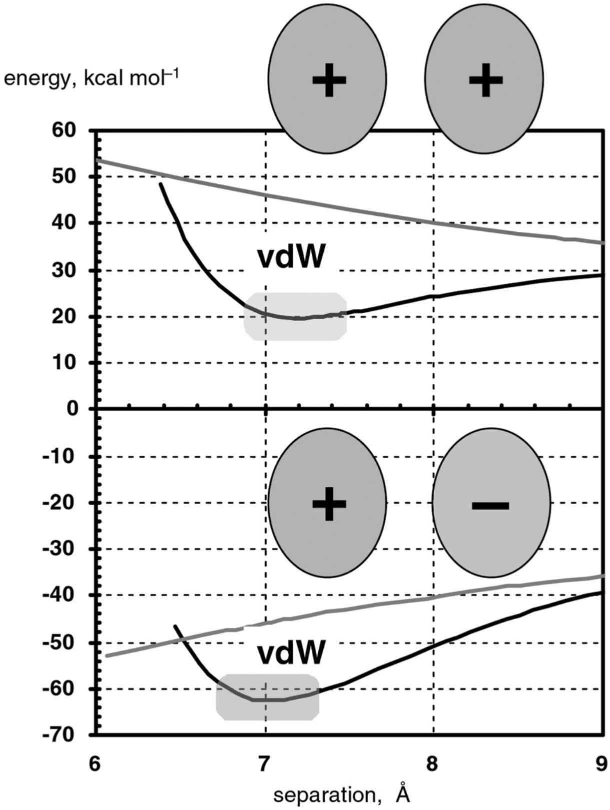

FIGURE 12 Diagrammatic representation of the intermolecular potentials for representative mono-charged polyatomic ions. The black curves represent total intermolecular potentials, and the red curves are the coulombic energies ($\varepsilon = 1$) for homo- and hetero-charged pairs. The green-shaded stabilisation for the hetero-charged pair is seen to exceed substantially the red-shaded destabilisation for the homo-charged pair.

hetero-charged pairs, the van der Waals energies (and associated polarisability enhancements) are always stabilising, such that the net intermolecular energy for a homo-charged pair could be of order $+20\,\mathrm{kcal\ mol^{-1}}$ (pink shaded region in Fig. 12), that for the hetero-charged pair could be of order $-60\,\mathrm{kcal\ mol^{-1}}$ (green shaded region), and the origin of the lattice energy is evident. This discussion is an extension of the classical Madelung calculation for crystals containing monatomic ions: a key additional concept is that as the size of a polyatomic ion increases, its electrostatic intermolecular energies decrease and its van der Waals intermolecular energies increase.

This discussion emphasises the importance of understanding the hierarchies of intermolecular energies in an aggregated system, such as a molecular crystal. The electrostatic energies for polyatomic ions such as commonly occur can be of order 50 kcal mol^{-1} (and much larger if doubly charged ions occur); a strong or charge-assisted hydrogen bond could contribute 15 kcal mol^{-1}; the water••water hydrogen bond contributes *ca*. 5 kcal mol^{-1}; a pair of benzene molecules or phenyl substituents could contribute 2 kcal mol^{-1}; and a pair of argon atoms (as representative of other similar sized atom pairs) contribute *ca*. 0.3 kcal mol^{-1}. Obviously it is important to recognise and understand the dominant influences in a crystal. This applies to both the analysis and interpretation of crystal packing, and to the design and eventual engineering of crystals. The DMol methodology can assist by providing potentials for relevant intermolecular interactions for any type of molecule.

SUMMARY AND CONCLUSIONS

I have drawn attention to questions and principles and concepts which I believe to be significant for the analysis, interpretation, and application of the packing of molecules in molecular crystals. I have described some systems which illustrate the multiple aryl embrace as a concerted intermolecular interaction, and the extension of this to the concept of a primary ⇒ secondary ⇒ tertiary ⇒ quaternary hierarchy of intermolecular structure in crystals. Some key properties of intermolecular energy, and associated concepts, are elaborated.

In summary, some salient principles are:

1. It is important to consider the complete structure of a molecular crystal, and all of intermolecular space.
2. Repeated and alternative crystallisations of molecular compounds are encouraged as routine procedures, in order to expand experimental knowledge of polymorph formation.
3. The almost unknown but potentially very informative realm of multi-component crystals is discussed. How might unusual crystals containing at least five different large molecules be grown?
4. Intermolecular OFF and/or EF aryl••aryl interactions occur in concert in multiple aryl embrace motifs, principally (OFF)(EF)$_2$, (EF)$_4$ and (EF)$_6$ embraces. These are well-established for phenylated molecules and metal coordination complexes. Embraces can be bimolecular or multimolecular, and embracing molecules can associate further in additional embraces, and thereby progress up the hierarchy of intermolecular structure.

5. High symmetry lattices for molecular crystals occur due to the repeated use of favourable intermolecular motifs.
6. An important concept for a molecular crystal is the asymmetric unit of intermolecular space. Crystals with large Z', in which the asymmetric unit of intermolecular space contains multiple molecules, could be regarded as having a number of polymorphs in the one crystal.
7. The general relationships between intermolecular potential and the van der Waals distance are described: for molecules without significant Lewis acid–base surface functionalities and hydrogen bonding capabilities, the majority of the structure-determining intermolecular interactions occur beyond the van der Waals distance, which is better regarded as a *lower* distance limit of informative interactions (rather than *upper* limit as is customary). For these molecular crystals the van der Waals criterion is the distance at which longer is stronger, and shorter is destabilising.
8. The distribution of immediate intermolecular distances reflects the intermolecular potential.
9. Informative intermolecular potentials can be calculated efficiently (for diverse chemical types) using density functional methods with the Perdew-Wang functional and numerical basis sets calculated over a large grid.
10. For typical charged polyatomic molecules the coulombic components of the energies are larger than the van der Waals components, and dominate the net intermolecular potential. Intermolecular potentials for embracing cations are calculated to be destabilising, and their observed occurrence is due to the greater stabilisation involving heterocharged polyatomic ions.

REFERENCES

[1] Dance, I. G. (1996). Supramolecular inorganic chemistry. In: *Perspectives in Supramolecular Chemistry*, Lehn, J. M. (Ed.), John Wiley: Chichester, Vol. 2, 137–233.

[2] Dance, I. (2003). Inorganic intermolecular motifs, and their energies. *Cryst. Eng. Comm.*, *5*, 208–221.

[3] Davey, R. J., Allen, K., Blagden, N., Cross, W. I., Lieberman, H. F., Quayle, M. J., Righini, S., Seton, L., & Tiddy, G. J. T. (2002). Crystal engineering – nucleation, the key step. *Cryst. Eng. Comm.*, *4*, 257–264.

[4] Evans, D. R., Fackler, N. L. P., Xie, Z., Rickard, C. E. F., Boyd, P. D., & Reed, C. A. (1999). π-Arene/cation structure and bonding. Solvation versus ligand binding in iron(III) tetraphenylporphyrin complexes of benzene, toluene, p-xylene, and [60]fullerene. *J. Am. Chem. Soc.*, *121*, 8466–8474.

[5] Dance, I. & Scudder, M. (1996). Supramolecular motifs: concerted multiple phenyl embraces between Ph_4P^+ cations are attractive and ubiquitous. *Chem. Eur. J.*, *2*,

481–486; Dance, I. (2004). π-π interactions: theory and scope, in: *Encyclopedia of Supramolecular Chemistry*, Atwood, J. L. and Steed, J. M., Eds., Dekker: New York, pp. 1076–1092.

[6] Dance, I. & Scudder, M. (1998). Supramolecular motifs: sextuple aryl embraces in crystalline [M(2,2′-bipy)$_3$] and related complexes. *J. Chem. Soc.*, *Dalton Trans.*, 1341–1350.

[7] Horn, C., Scudder, M. L., & Dance, I. G. (2001). Contrasting crystal supramolecularity for [Fe(phen)$_3$] I$_8$ and [Mn(phen)$_3$] I$_8$: complementary orthogonality and complementary helicity. *Cryst. Eng. Comm.*, *3*, 1–8.

[8] Dance, I. & Scudder, M. (1996). Concerted supramolecular motifs: linear columns and zig-zag chains of multiple phenyl embraces involving Ph_4P^+ cations in crystals. *J. Chem. Soc.*, *Dalton Trans.*, 3755–3769.

[9] Alyea, E. C., Fisher, K., Scudder, M., Craig, D., & Dance, I. (2003). Ph_4P^+ oxomolybdates paper. Unpublished.

[10] Scudder, M. L., Goodwin, H. A., & Dance, I. G. (1999). Crystal supramolecular motifs: two-dimensional grids of terpy embraces in $[ML_2]^z$ complexes (L = terpy or aromatic N$_3$-tridentate ligand). *New J. Chem.*, *23*, 695–705; McMurtrie, J. & Dance, I. G. (2003). Terpy embrace motifs. To be published.

[11] Hasselgren, C., Dean, P. A. W., Scudder, M. L., Craig, D. C., & Dance, I. G. (1997). Dominant cation–cation supramolecular motifs in crystals. Hexagonal arrays of sextuple phenyl embraces in halometallate salts of $MePh_3P^+$.*J. Chem. Soc.*, *Dalton Trans.*, 2019–2027; Scudder, M. & Dance, I. (1998). Crystal supramolecularity. Hexagonal arrays of sextuple phenyl embraces amongst chemically diverse compounds. *J. Chem. Soc.*, *Dalton Trans.*, 329–344.

[12] Dance, I. & Scudder, M. (1998). Crystal supramolecularity: elaborate 6-, 8-, and 12-fold concerted phenyl embraces in compounds $[M(PPh_3)_3]^z$ and $[M(PPh_3)_4]^z$. *New J. Chem.*, *22*, 481–492; Scudder, M. & Dance, I. (1998). Crystal supramolecular motifs. Ladders, layers and labyrinths of Ph_4P^+ cations engaged in fourfold phenyl embraces. *J. Chem. Soc.*, *Dalton Trans.*, 3155–3166; Scudder, M. & Dance, I. (1998). Crystal supramolecular motifs. Two- and three-dimensional networks of Ph_4P^+ cations engaged in sixfold phenyl embraces. *J. Chem. Soc.*, *Dalton Trans.*, 3167–3176; Dance, I. G. & Scudder, M. L. (2000). Crystal supramolecularity: sixfold phenyl embraces between PPh$_3$ ligands, forming extended nets in one-, two-, and three-dimensions. *J. Chem. Soc.*, *Dalton Trans.*, 1587–1594; Russell, V. M., Craig, D. C., Scudder, M. L., & Dance, I. G. (2000). Interpenetrating non-molecular and supramolecular (10,3)-a nets occur with chiral recognition in crystalline (Ph$_3$MeP)$_2$[NaCr(ox)$_3$]. *Cryst. Eng. Comm.*, *2*, 16–23; Dance, I. G. & Scudder, M. L. (2001). A diamondoid supramolecular crystal lattice maintained entirely by sixfold phenyl embraces. *Cryst. Eng. Comm.*, *3*, 46–49.

[13] Horn, C., Dance, I. G., Craig, D., Scudder, M. L., & Bowmaker, G. A. (1998). A short but weak Cu–Cu interaction in $[Cu_2Br_5]^{2-}$, a crystal engineered $(Cu^{+1.5})_2$ confacial bitetrahedral complex. *J. Am. Chem. Soc.*, *120*, 10549–10550.

[14] Dance, I. G. & Scudder, M. L. (2001). High symmetry crystal supramolecularity: –XPh$_3$ molecules in cubic lattices. *New J. Chem.*, *25*, 1500–1509; Dance, I. G. & Scudder, M. L. (2001). High symmetry crystal supramolecularity: –XPh$_3$ molecules in rhombohedral lattices, using multimolecular rather than bimolecular sixfold phenyl embraces. *New J. Chem.*, *25*, 1510–1515.

[15] Steed, J. W. (2003). Should solid-state molecular packing have to obey the rules of crystallographic symmetry? *Cryst. Eng. Comm.*, *5*, 169–179.

[16] Jacobsen, H., Schmalle, H. W., Messmer, A., & Berke, H. (2000). Remarkable low symmetry hydrogen bonding network in the structure of $ReCl_2(NCMe)(NO)(PMe_3)_2$. *Inorg. Chim. Acta*, *306*, 153–159.

[17] Jeffrey, G. A. (1997). An Introduction to hydrogen bonding. In: *Topics in Physical Chemistry*, Truhlar, D. G. (Ed.), Oxford University Press: New York; Desiraju, G. R. & Steiner, T. (1999). In: *The Weak Hydrogen Bond in Structural Chemistry and Biology*, (Ed.), Oxford University Press: Oxford; Desiraju, G. R. (2000). Hydrogen bonds and other intermolecular interactions in organometallic crystals. *J. Chem. Soc.*, *Dalton Trans.*, 3745–3751; Steiner, T. (2002). The hydrogen bond in the solid state. *Angew. Chem. Int. Ed. Engl.*, *41*, 48–76; Desiraju, G. R. (2002). Hydrogen bridges in crystal engineering: interactions without borders. *Acc. Chem. Res.*, *35*, 565–573; Gavezzotti, A. (2002). Modeling hydrogen bonded crystals. *J. Molec. Struct.*, *615*, 5–12.

[18] Dance, I. (2003). Distance criteria for crystal packing analysis of supramolecular motifs. *New J. Chem.*, *27*, 22–27.

[19] Rowland, R. S. & Taylor, R. (1996). Intermolecular non-bonded contact distances in organic crystal structures: comparison with distances expected from van der Waals radii. *J. Phys. Chem.*, *100*, 7384–7391.

[20] Delley, B. (1990). An all-electron numerical method for solving the local density functional for polyatomic molecules. *J. Chem. Phys.*, *92*, 508–517.

[21] Delley, B. (1995). DMol, a standard tool for density functional calculations: Review and advances. In: *Theoretical and computational chemistry*, Politzer, P. & Maksic, Z. B. (Eds.), Elsevier: Amsterdam, Vol. 2, 221–254; Delley, B. (2000). From molecules to solids with the DMol3 approach. *J. Chem. Phys.*, *113*, 7756–7764.

[22] Wesolowski, T. A., Parisel, O., Ellinger, Y., & Weber, J. (1997). Comparative study of benzene···X ($X = O_2$, N_2, CO) complexes using density functional theory – the importance of an accurate exchange-correlation energy density at high reduced density gradients. *J. Phys. Chem.*, *101*, 7818–7825.

[23] Perdew, J. P. & Wang, Y. (1992). Accurate and simple analytic representation of the electron-gas correlation energy. *Phys. Rev. B*, *45*, 13244–13249.